

Impurity transport in the W7-AS stellarator

R. Burhenn, J. Baldzuhn, R. Brakel, H. Ehmler, L. Giannone, P. Grigull, J. Knauer, M. Krychowiak, M. Hirsch, K. Ida¹, H. Maassberg, K. McCormick, E. Pasch, H. Thomsen, A. Weller, W7-AS team, ECRH group², NI group

Max-Planck-Institut für Plasmaphysik, EURATOM-Ass., D-17491 Greifswald, Germany

¹National Institute for Fusion Sciences, Toki, Gifu 509-5292, Japan

²Institut für Plasmaforschung, Universität Stuttgart, D-70569 Stuttgart, Germany

Abstract

The dependence of impurity transport on plasma parameters such as density, heating power, magnetic field strength and the isotope composition of the working gas was investigated by means of laser blow-off technique. Additional to the global confinement time, also local transport coefficients were derived. An increased transport at higher heating power and lower magnetic field strength as well as no effect of the isotope composition on the confinement was observed. The unfavourably increasing confinement of impurities towards higher densities turned out to be the most critical scaling which limited the maintenance of stationary conditions within the pulse length at high density. Therefore, this point was elucidated in more detail. In particular, high density neutral beam heated plasmas often suffered from degradation of plasma energy due to an increasing radiation level and by loss of density control. This was addressed to a reduction of the impurity diffusion coefficient with density. Nevertheless, after installation of the new island divertor modules, the plasma abruptly changed its confinement properties and switched from Normal Confinement (NC) into the High Density H-mode (HDH) at a certain power dependent threshold density. This transition is characterized by a strong reduction of the impurity confinement time and an increase in energy confinement time while the density profiles changes from a peaked to a flat one. In the HDH operational regime, access to even higher densities than achieved before became possible under stationary operation conditions. Impurity transport measurements and model predictions indicate, that the reduction of the impurity confinement in HDH is not only caused by a reduction of the inward convection in the core plasma but possibly also by changes in the edge transport.

1. Introduction

The study of transport behaviour of intrinsic impurity ions in fusion plasmas is a long standing field of research. Nevertheless, the importance to prevent impurity accumulation in improved energy confinement regimes in order to maintain stationary plasma conditions is still one of the key questions in fusion research and remains an indispensable part of the ongoing investigations. In tokamaks, the appearance of e.g. edge localized modes or saw-tooth crashes, which originally are confinement degrading phenomena, are actively used to flush out impurities. Stellarators are free of externally induced currents and, consequently, cannot utilize current-connected phenomena like saw-toothing for impurity reduction. Due to the existence of a quite different magnetic topology compared to tokamaks, certain additional transport regimes in the long mean free path regime exists in stellarators [1] which might also affect the impurity transport in the plateau or Pfirsch-Schlueter regime (e.g. temperature screening). The study of impurity transport in stellarators is therefore an urgent need, in particular, because the data base in this field is by far not as large for stellarators as for

tokamaks. Especially, at large stellarator devices which should demonstrate quasi-stationary plasma operation the study of impurity transport is a matter of special interest /2/. The key question is to what extent the impurity behaviour can be described by existing theoretical models (neo-classical and Pfirsch-Schlueter model) which, are mainly based on formalisms specific to axisymmetric devices. In the case of agreement with the theoretical model, the observed transport features are understood and conclusions can be drawn with respect to further improvements and extrapolations. If the confinement is dominated by turbulent transport, further interpretation becomes difficult and predictions have to be substituted by measurements.

For this reason, parameter studies were performed at W7-AS in order to elucidate the various dependences of impurity transport on e.g. heating power, magnetic field strength, isotope effect or density. Additionally, they were compared to model predictions in order to ascertain the contribution of the theoretically expected transport to the observed global confinement.

2. Experimental set-up

The impurity transport in W7-AS was investigated by means of laser blow-off technique (LBO), mostly with aluminium but also with other tracer material. The temporal behaviour of different ionization states of the tracer ions in the plasma after the injection was monitored by VUV spectrometers in the case of lower ionization states (Al IX-XI) and a crystal spectrometer for the highest ionization states (Al XII-XIII) – all with central line-of-sight. The impurity confinement time as a global transport quantity was derived from the temporal decay of the radiation emitted by the highest states. The local transport quantities were evaluated by an iterative procedure /3/ from the temporal and spatial radiation evolution after the injection obtained from the soft-X camera system with 25 microns Be as filters. Additionally, C⁶⁺ density profiles at the plasma edge were provided by Li-beam CXS measurements. For comparison with theoretical predictions, the impurity transport code SITAR /4/ was used, which is based on the neoclassical and Pfirsch-Schlueter model for axisymmetric devices. Stellarator specific features of impurity transport are not implemented.

3. Experimental Results

3.1 Impurity transport in ECRH plasmas

ECRH plasmas in W7-AS were typically heated by 140 GHz (2nd harmonic X-mode) or 75 GHz (1st harmonic O-mode) ECF waves which are absorbed in a small resonance layer at the radial location of the plasma center where the magnetic field strength is 2.5T. Towards high densities, this type of heating mechanism is limited by the cut-off frequency for 140 GHz of approximately $1.2 \times 10^{20} \text{ m}^{-3}$. Higher densities can only be achieved by non-resonant heating methods like neutral beam injection (NBI) which is described later. In the following section the impurity transport in ECRH plasmas was investigated. From aluminium laser blow-off experiments in ECRH-plasmas under different conditions, a scaling law for the impurity confinement time $\tau_{\text{Al}} \sim a_p^{2.4} n_c^{1.2} / P_{\text{ECRH}}^{0.8}$ was derived for plasmas with central densities lower than $5 \times 10^{19} \text{ m}^{-3}$ /5/. Surprisingly, besides the strong dependence on plasma size, heating power and density, the magnetic field strength seems not to play an important role for the impurity transport. Additionally, no isotope effect was observed and only a weak dependence on the rotational transform /6/. The observed dependencies are not trends which are typically expected from the neo-classical and Pfirsch-Schlueter transport model and therefore points to the additional presence of anomalous transport.

3.1.1 Dependence on magnetic field strength

In order to investigate the nearly missing dependence of the impurity confinement time on the magnetic field strength B ($\sim B^{0.3}$) - which is not understandable at all in the picture of both, the theoretical transport model as well as the anomalous transport - two plasmas at 2.5T and 1.25T central magnetic field strength were compared. In order to be independent from the central resonance condition in the case of ECRH heating when operating at two different central magnetic field strengths, NBI-heating had to be applied. Unfortunately, both discharges (central density $8 \times 10^{20} \text{m}^{-3}$, $\tau=0.35$, $P_{\text{NBI}}=500 \text{ kW}$) could not be sufficiently tailored in order to achieve completely identical temperature and density profiles. Among other things, the reason for this was obviously the existing dependence of the energy confinement time on the magnetic field strength. Nevertheless, the local impurity diffusion coefficient D in the plasma core actually reveals significantly larger values in the case of 1.25T compared to 2.5T (factors of 3-4) – as predicted by theory. However, the inward convection v is also increased, so that in total the global impurity confinement time do not change in these two cases [7] - as being experimentally observed. Whether this result has a general character and can be used to explain the missing sensitivity on B in the confinement time scaling law is not quite clear.

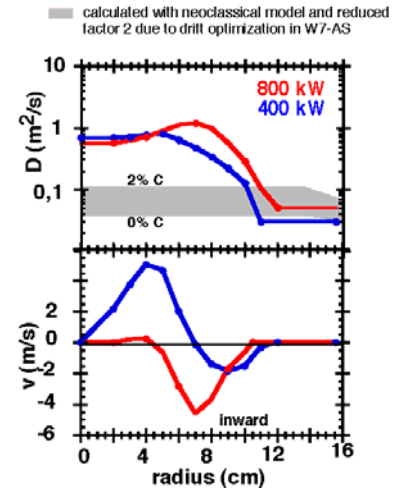


Fig.1: Effect of ECRH-heating power on transport coefficients. Shaded area: model predictions with different assumptions about impurity background level.

3.1.2 Dependence on heating power

Comparison of discharges with similar central density ($4 \times 10^{20} \text{ m}^{-3}$), magnetic field strength (2.5T) and edge rotational transform ($\tau = 0.35$) but different ECRH heating power (400kW/800kW) show a degradation of impurity confinement at higher heating power. This manifests itself in shorter decay times after impurity injection by laser blow-off as well as in enhanced diffusion coefficients D throughout the entire plasma cross section (Fig.1). This might be an indication for enhancement of turbulent transport at increased heating power.

3.1.3 Dependence on plasma density

The most important impact on impurity transport with respect to its consequences on the machine performance is given by the unfavourable density dependence of the impurity confinement time. At high density (e.g. $7.5 \times 10^{19} \text{ m}^{-3}$) the confinement time can reach values close to a second or even more. Stationary radiation levels can usually be sustained at low density without problems. Beyond a central density of approximately $5 \times 10^{19} \text{ m}^{-3}$ the intrinsic impurity radiation as well as Z_{eff} start

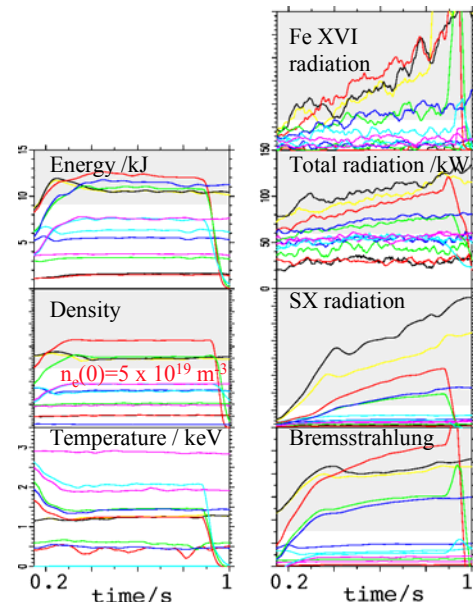


Fig.2: Behaviour of intrinsic impurity radiation in discharges with different density: increase of radiation for central densities $> 5 \times 10^{19} \text{ m}^{-3}$ (grey area).

continuously to rise throughout the pulse length. Depending on the flux level from the walls, this can lead to a degradation of the plasma energy by radiation losses at highest density. The important question arise whether this effect is a consequence of changes in transport – which is indeed indicated by the long confinement times – or the result of temporally increasing impurity sources from the wall (e.g. heating up of inboard tiles). This will be elucidated in the following chapters.

3.1.3.1 Difference in local transport

In order to study the effect of increasing intrinsic impurity radiation during the pulse duration at high density, the local transport coefficients were derived and compared (Fig.3) for a low central density ($3.5 \times 10^{19} \text{ m}^{-3}$) and a high central density ($7 \times 10^{19} \text{ m}^{-3}$) plasma /8/ ($t=0.35$, $B=2.5\text{T}$, $P_{\text{ECRH}} = 400\text{kW}$). In the case of high density a clear overall reduction of D by a factor of approximately 3 was found with comparable convective velocities. Beyond $r=12\text{cm}$, the soft-X camera signals

were too low in order to continue the analysis. Therefore, some kind of constant “effective diffusion coefficients” as well as a meaningful convection velocity were extrapolated which finally match the time behaviour (increase, decay and radial profile of soft-X camera) of the spectroscopic signals. In the case of low density, the fast onset of a stationary radiation level (Fig.3, right, red) can be well described by the existence of a higher diffusive transport which leads to a shorter time scale for achieving stationarity. The observed increase of radiation at high density (Fig.3, right, blue) is compatible with the lower diffusion coefficients, in particular at the edge. As a consequence, the reduced impurity fluxes cause a longer time scale for achieving stationary conditions within the discharge duration (in Fig.3: stationarity is predicted to be achieved at approximately 1.7s in the high density case - longer than the pulse length). Therefore, the different time behaviours of the intrinsic impurities could principally be purely explained by changes in transport.

3.1.3.2 Effect of transient sources on impurity behaviour

In order to exclude the effect of transient impurity sources on the increasing impurity behaviour at high density, a constant fluorine gas puff (CHF_3) was applied throughout the pulse duration of a high density discharge (comparable

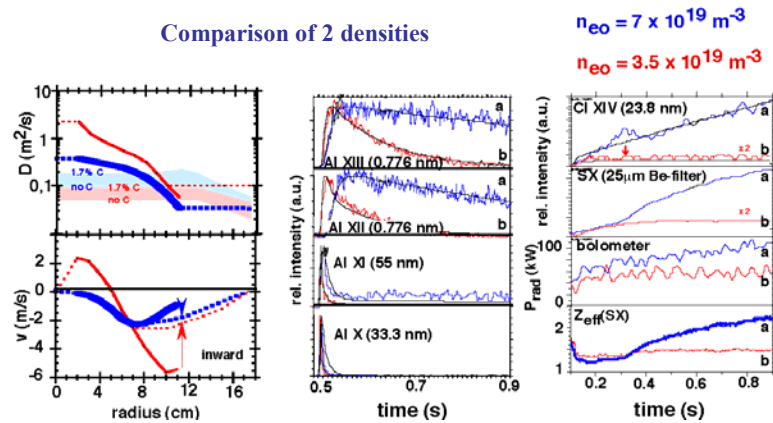


Fig.3: left: transport coefficients in a high (blue line) and low (red line) density ECRH plasma and model predictions (shaded area); time traces of aluminium radiation after LBO (middle) and intrinsic impurity radiation (right) together with simulations using the D, v -profiles (left).

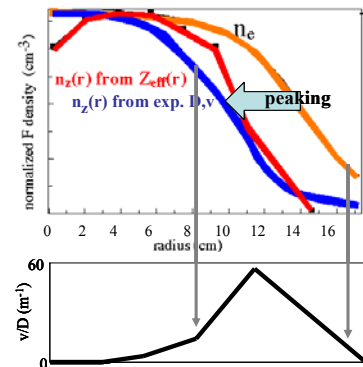


Fig.4: Fluorine density profiles in a high density ECRH plasma after 1s constant fluorine influx normalized to the electron density profile: from Z_{eff} -profile (red) and from prediction using the derived D, v values from Fig.3 (blue)

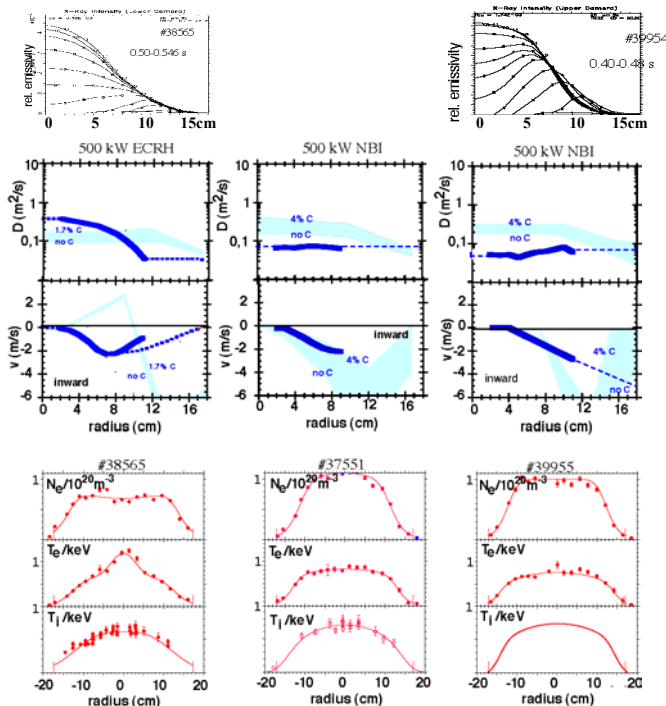
to that in Fig.3) [7], simulating a stationary impurity source. The temporal behaviour of the fluorine radiation measured by soft-X camera was extracted by subtracting discharges with/without fluorine gas puffing. In spite of the constant impurity influx, the fluorine radiation in the plasma core starts indeed continuously to rise, up to the end of the pulse – indicating an accumulation of fluorine in the core plasma. This supports the previous result, that not transient sources but transport is responsible for the unfavourable intrinsic impurity behaviour at high density. A closer look to the fluorine density profiles at the end of the pulse reveals – for the profile predicted by SITAR using the experimentally derived transport coefficients as well as the fluorine density profile obtained from the difference in the Z_{eff} -profile – a clear peaking with respect to the electron density profile (Fig.4, top). This peaking occurs mainly in the outer half of the plasma, where the contribution of the inward convection exceed the diffusive fraction (Fig.4, bottom)).

3.2 Impurity transport in NBI plasmas

ECRH heating is only applicable up to the cut-off frequency of $1.2 \times 10^{20} \text{ m}^{-3}$ for 140 GHz gyrotron frequency. Access to higher densities is only possible by NBI heating. Comparison of ECRH- and NBI-heated plasmas in the overlapping high density region show similar and extremely long impurity confinement times.

3.2.1 Comparison: ECRH plasmas – NBI plasmas

In spite of similar long impurity confinement times, there are typical differences in the radial profiles of the local transport parameters for both heating scenarios. ECRH heated plasmas reveal high diffusion coefficients in the central plasma region with low values at the plasma edge, whereas NBI-heated plasmas exhibit rather flat D-profiles with strongly increasing inward convection v towards the plasma boundary (Fig.5, middle). This is mirrored in the temporal evolution of the radial soft-X radiation after laser blow-off injection of aluminium (Fig.5, top): once the injected impurities passes the plasma edge – which, determines completely the time constant of the penetration process like a bottle neck - they spread out



very quickly over the central region of the plasma in the case of ECRH-heating. In NBI heated plasmas the impurity density front moves slowly towards the plasma center, pointing

Fig.5: comparison of ECRH (left) and NBI (right two ones) heated plasmas; top: temporal evolution of the soft-X radiation profile after LBO; middle: comparison of experimental (blue lines) and predicted (blue shaded area) local transport coefficients; bottom: profiles of plasma density and -temperature

to a low and flat diffusion coefficient but also to a high inward velocity (Fig.5, top). Of course, it

should be mentioned, that these figures show only the radiation – not the density. But, nevertheless, they might be useful to point up the differences in the penetration process, which is almost predicted by the profiles of the local transport coefficients (Fig.5, middle).

The figures of the local transport coefficients for the injected aluminium in Fig.5 (middle) contain also predictions by the transport model (blue shaded area). The lower limit is given by the case without any consideration of an additional background impurity, whereas the upper limit represents the case taking a certain carbon concentration into account (carbon is assumed to be the most prominent species in W7-AS), which approximately meets the measured Z_{eff} . The comparison of the predicted and measured diffusion coefficients points up a discrepancy by a factor of 3-8. At present, it is not clear whether this deviation is a problem of stellarator specific features, which are not considered in the existing model.

3.2.2 Divertor operation

Fig.6 shows the dependence of the impurity and energy confinement time on plasma density for different heating scenarios (pure ECRH, pure NBI, combined heating ECRH+NBI). The previously mentioned unfavourable scaling of the impurity confinement time on the density was obtained in ECRH plasmas (yellow region). Going to higher density (green region) a similar trend of the impurity confinement time on density was found also for NBI plasmas. Unfortunately, they were often characterized by impurity accumulation and loss of density control at the highest densities.

Since W7-AS had been equipped with new island divertors, a new operational regime for high density operation became accessible – the High Density H-mode, HDH /9,10/). This regime allows access to densities up to $4 \times 10^{20} \text{ m}^{-3}$ under stationary conditions.

3.2.3 The HDH regime

When approaching a certain NBI heating power dependent threshold density, the impurity confinement time drops sharply down to values comparable to the energy confinement time (Fig.6). To the same time the energy confinement time rises by nearly a factor of 2. Unlike the impurity behaviour in normal confinement (NC) plasmas, the degraded impurity confinement in HDH now permits access to stationary high density

Fig.7: top: transport coefficients for a NC and HDH plasma with 1 MW NBI heating power. The coloured region is the confinement region of the plasma with separatrix around 14cm. bottom: density and temperature profiles of NC and HDH plasmas

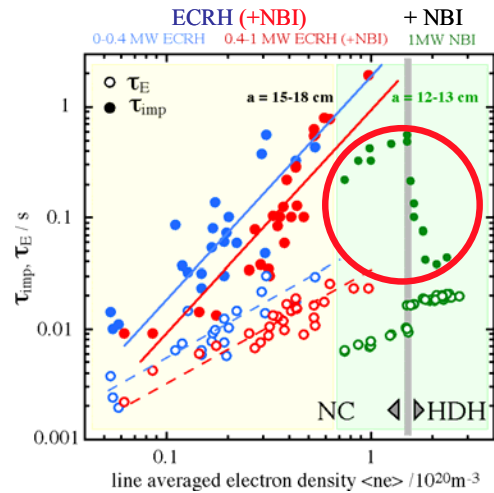
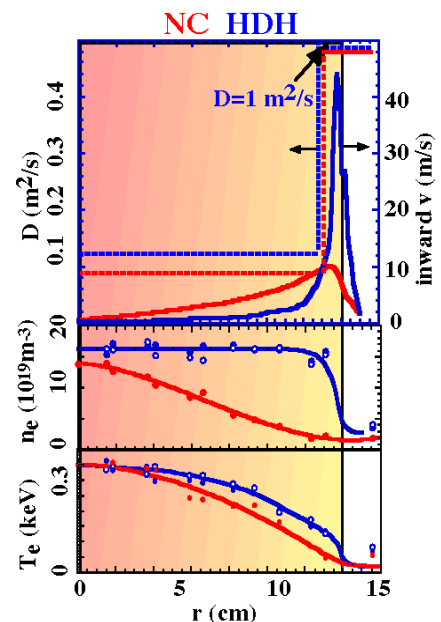


Fig.6: Energy and impurity confinement times vs. electron density for normal confinement (NC) limiter ECRH plasmas (yellow region) and NBI plasmas (green region) including the HDH transition during divertor operation.



operation up to densities of $4 \times 10^{19} \text{ m}^{-3}$. At the transition from NC to HDH operation, the plasma density profile changes from a peaked one to an extremely flat profile with steep edge gradients (Fig.7). The plasma temperature profile does not essentially change. At present, the reason for the sudden transition is not clear and subject of ongoing investigations. One of the most urging questions is, whether the change in impurity confinement can be explained by the transport model as a consequence of the changing plasma profiles.

3.2.3.1 Differences in local transport

Laser blow-off transport analysis using a simple transport model ($D(r)=\text{const}$, $v(r)=v(a)(r/a)$) reveals that the degraded impurity confinement in HDH is the consequence of a reduced inward convection /11/, whereas the diffusion coefficient does not change very much. More refined analysis methods /11,12/ provide the same result as far as the core plasma is concerned. At first glance, it seems to be obvious to explain the degraded confinement in terms of the neo-classical and Pfirsch-Schlueter transport model: the flattening of the density profile in HDH reduces the central inward velocity drastically in the presence of nearly comparable temperature screening due to similar temperature profiles in NC and HDH.

However, the detailed analysis of the radial profiles of D and v /11,12/ reveals for the plasma edge additionally a strongly increasing inwards convective velocity in HDH (Fig.7). In spite of the reduced central inward convective velocity, the enhanced inward velocity layer at the plasma edge infers long confinement times – which is in contradiction to the observations. Consequently, an artificially enhanced diffusive transport layer had to be introduced at the plasma edge (in the region of the high inward convection layer) in order to match the short experimental confinement times in HDH.

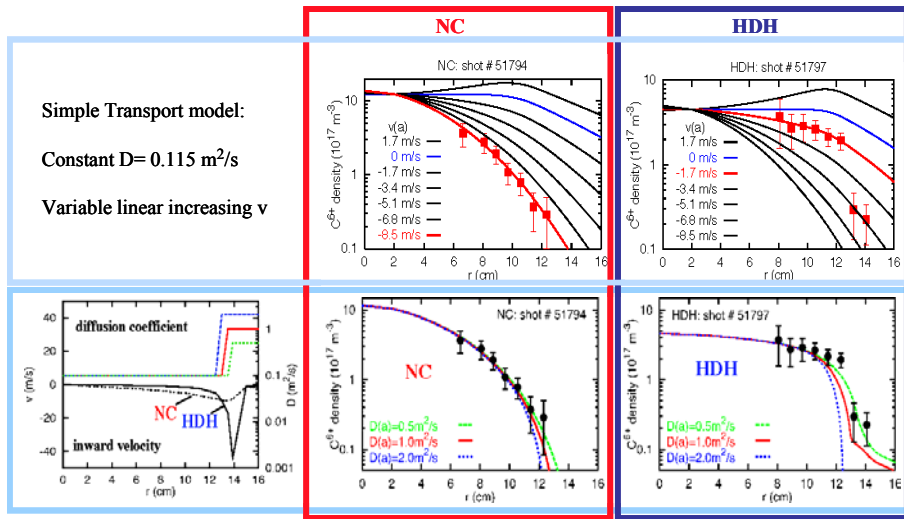


Fig.8: Simulation of C^{6+} density profiles measured in a 1MW NBI heated NC and HDH plasma: a) using a simple transport model (top); b) using the D, v profiles (left side) similar to Fig.7 (bottom).

Indications, that such an enhanced edge transport might be realistic, is given by Li beam-CXS measurements of C^{6+} density profiles in NC and HDH as shown in Fig.8. In HDH, the step-like structure of the C^{6+} density profile at the plasma edge can be more successfully reproduced using the transport coefficients (bottom, left) similar to that of Fig.7 than using a simple transport model ($D(r)=\text{const}$, $v(r)=Cx(r/a)v(a)$) /13/. The location of the step corresponds spatially to the onset of the high diffusive edge layer.

Although there is still no definit evidence for enhanced turbulent transport or mode activity at the plasma edge, the strong sensitivity of the impurity confinement on the existence of such a diffusive layer points to the key role of edge transport for the global confinement properties of impurities – additionally to the existing core transport. This assumption is supported by the confinement properties in the H^* mode /14,15/ which appears at densities slightly lower than

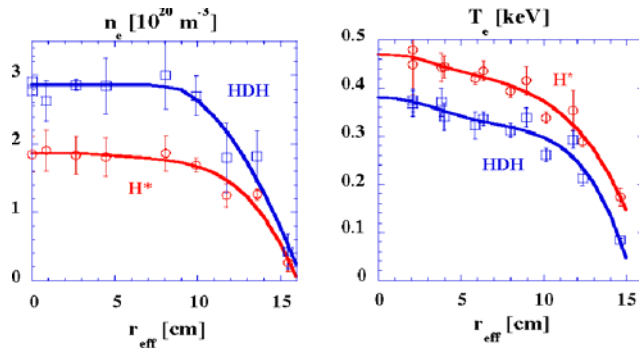


Abb.9: Radial profiles of electron temperature and density within in a discharge where the HDH-mode is established starting from a previous H*-mode by slightly rising the density.

the threshold density for the NC/HDH transition. In spite of small differences in the value of the central density, their density as well as the electron temperature profiles in HDH and H* are comparable (Fig.9) /15/. Nevertheless, compared with the HDH mode, which has a strongly degraded impurity confinement, the H* mode reveals an extremely good confinement (Fig.10) /16/. This contradiction cannot easily be resolved by assigning the different transport to a change of the central density profile. Obviously, this is another indication that not exclusively the core plasma is responsible for the

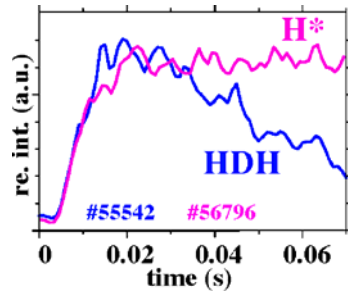


Abb.10: The H*-mode is characterized by long impurity confinement times compared to the strongly reduced confinement in HDH.

global impurity confinement but, moreover, additionally the edge plasma properties. Unfortunately, possible differences in the edge profiles could not be measured with the precision, necessary for a clear interpretation.

3.2.3.2 Model predictions

In order to see to what extent the observations can be predicted by the theoretical transport model, calculations were done with different assumptions about the level of the background impurity concentration (Fig.10, left and middle) /16/. Surprisingly, the results of the predicted transport coefficients show remarkably similarities to the experimentally derived ones in Fig.7 – both, in quantity and quality (in particular, the strong rise in the edge inward convective velocity in HDH). Consequently, the simulated time traces of Al X-XII (Fig.10, right) show long decay times for NC (as expected: due to the high central inward convective velocity) as well as for HDH (due to the strong edge inward velocity). The only way to match the short

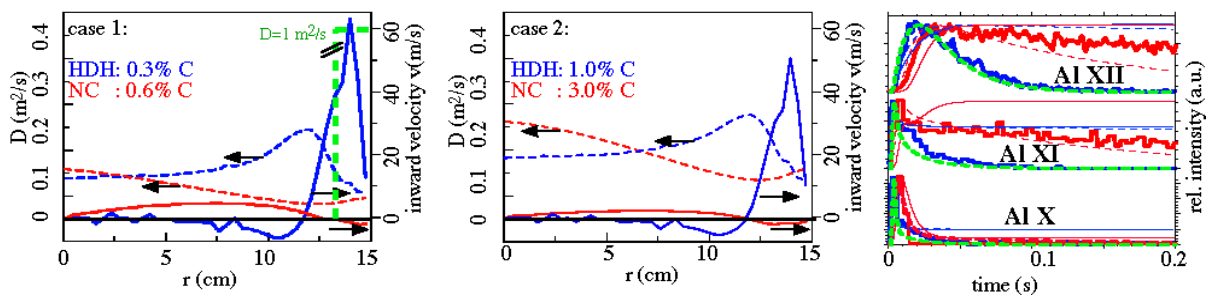


Fig.10: Predictions from neo-classical and Pfirsch-Schlueter model for HDH (always blue) and NC (always red). Left and central figure: diffusion coefficient D (broken lines), inward convective velocity (solid lines). Right figure: Al X-XII line radiation after Al laser blow-off (thick solid lines) and predictions for case 1 (thin solid lines) and case 2 (thin broken lines). The green fit is the result of the introduction of an additional enhanced edge transport (left: green curve).

experimental confinement time in HDH was the introduction of an edge layer with enhanced diffusion (Fig.9, green curves). This means, that – with the exception of the enhanced edge diffusion – the transport in both regimes at these high densities is close to that predicted by the theoretical transport model.

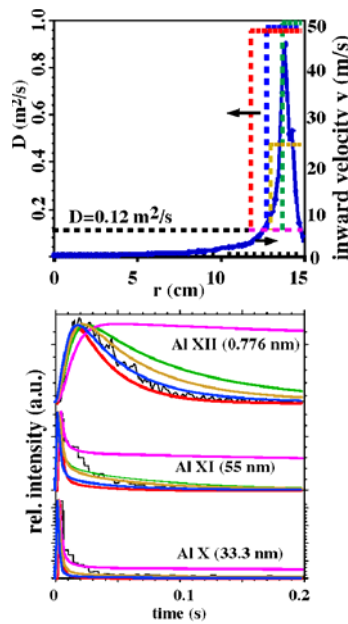


Abb.11: Dependence of impurity confinement time of laser blow-off injected aluminium (bottom) on the extension and strength of the anomalous high diffusive layer (top).

If the introduction of the edge layer with enhanced diffusive transport is able to change completely the confinement situation, it is interesting to elucidate the sensitivity of the confinement on the size and the spatial extension of this layer. In Fig.11 is shown that nearly any decay time constant can be predicted when changing the size and extension of this zone. The reason for this high sensitivity is that also the region of high edge inward velocity is only a small layer. Because both layers have the reversed effect on the confinement, their relative location and overlap determines how effective they can counteract each other. Consequently, each change in transport in this edge localized region – either by turbulent transport, mode activity, frequent ELM activity or other mechanisms which are represented now by the artificially introduced enhanced edge diffusion – will affect the global impurity confinement.

With respect to these results, it can be assumed that the striking difference in the impurity transport behaviour between H*- and HDH mode must not necessarily be a contradiction but might be attributed to changes of anomalous transport properties at the edge.

4. Summary

Electron cyclotron radiation (ECR) -heated plasmas in the stellarator Wendelstein 7-AS with limiter configuration reveal a strong dependence of the aluminium confinement time on minor radius a_p , heating power P_{ECRH} and plasma density n_e ($\tau_{\text{Al}} \sim a_p^{2.4} n_e^{1.2} / P_{\text{ECRH}}^{0.8}$). Towards higher heating power, the diffusion coefficient becomes larger over the entire plasma, leading to a degeneration of impurity confinement. No isotope effect was observed. Plasmas with lower magnetic field strength reveal a larger diffusion coefficient but, however, also a higher inward convection velocity. Consequently, nearly no difference in the confinement time was found in the two discharges under consideration. Stationary radiation levels can usually be sustained at low density, whereas the increasing impurity confinement at higher densities ($> 5 \times 10^{19} \text{ m}^{-3}$) causes a rise in impurity radiation throughout the pulse duration. This behaviour is ascribed to a reduced diffusion coefficient at higher density and the related longer time scale necessary to achieve stationary impurity profiles. Nevertheless, the derived scaling is not in agreement with the existing transport model and points to the presence of anomalous transport.

The investigation of impurity transport at densities higher than the cut-off frequency of the ECR heating systems ($1.2 \times 10^{20} \text{ m}^{-3}$) is restricted to neutral beam injection (NBI) heated plasmas. They are also characterized by long impurity confinement times, low diffusion coefficients and additionally high inward convection, often suffering from a loss of density control and a degradation of plasma energy by radiation losses. The observed density dependence of the confinement as well as the absolute values of the transport coefficients are not compatible with neoclassical (and Pfirsch-Schluter) predictions. Differences in transport

between H-mode and L-mode plasmas are difficult to extract, because at densities where the H-mode usually appears, the impurity confinement time of the L-mode plasma is already large.

Operation with the new island divertor modules permits densities up to $4 \times 10^{20} \text{ m}^{-3}$. Beyond a certain power dependent threshold density ($1.5\text{-}2.1 \times 10^{20} \text{ m}^{-3}$), the unfavourable density scaling of impurity confinement in the normal confinement regime (NC) suddenly changes. Within a small density interval, the plasma enters the High Density H-mode (HDH) regime and the confinement time drops to values comparable to the energy confinement time, which simultaneously increases by nearly a factor of 2. As a result, the HDH-mode provide quasi-stationary operation at densities up to $4 \times 10^{20} \text{ m}^{-3}$.

The drop in impurity confinement in HDH is in agreement with the observed reduction of the inward convection in the core (which might be related to the flattening of the density profiles) but is in contradiction to the strong inward convection at the plasma edge. Comparison with the H*-mode, having nearly similar profiles than HDH but a good impurity confinement, points to the importance of edge transport.

References:

- /1/ A.A. Galeev, R.Z. Sagdeev, 1979, Reviews of Plasma Physics Vol.7, Leontovich M.A., Editor, (Consultants Bureau, New York)
- /2/ Y. Nakamura et al., Proc. 28th EPS Conference, Funchal 2001, ECA Vol. 25A, P4.041
- /3/ R. Burhenn, A. Weller, Rev. Sci. Instrum., Vol. 70, No.1 (1999)
- /4/ W VII-A Team et al., Nucl. Fus., Vol.25, No.11 (1985)
- /5/ R. Burhenn et al., Proc. 22th EPS Conference, Bournemouth 1995, **19C**, part III, 145
- /6/ R. Brakel, R. Burhenn et al., Proc. 20th EPS Conference, Lissabon 1993, **17C**, part I, 361
- /7/ R. Burhenn et al., Proc. 27th EPS Conference, Budapest 2000, ECA Vol. 24B, P3.041
- /8/ R. Burhenn et al., Proc. 24th EPS Conference, Berchdesgaden 1997, **21A**, part IV, 1609
- /9/ K. McCormic et al., Phys. Rev. Lett. 89 (2002) 015001-1
- /10/ R. R. Jaenicke et al., Plasma Phys. Control. Fusion, **44**, (2002), B193
- /11/ R. Burhenn et al., Proc. 29th EPS Conference, Montreaux 2002, ECA Vol. 26B P.4.043
- /12/ K. Ida et al., Plasma Phys. Control. Fusion 45 No.10 (2003) 1931-1938
- /13/ H. Ehmler et al., Proc. 29th EPS Conference, Montreaux 2002, ECA Vol. 26B P.4.044
- /14/ K. McCormick et al., J.Nucl. Mater. 313-316 (2002) 1131
- /15/ K. McCormick et al., Proc. 30th EPS Conference, St.Petersburg 2003, P-1.1
- /16/ R. Burhenn et al., Proc. 30th EPS Conference, St.Petersburg 2003, P-1.2